

Supplemental Data

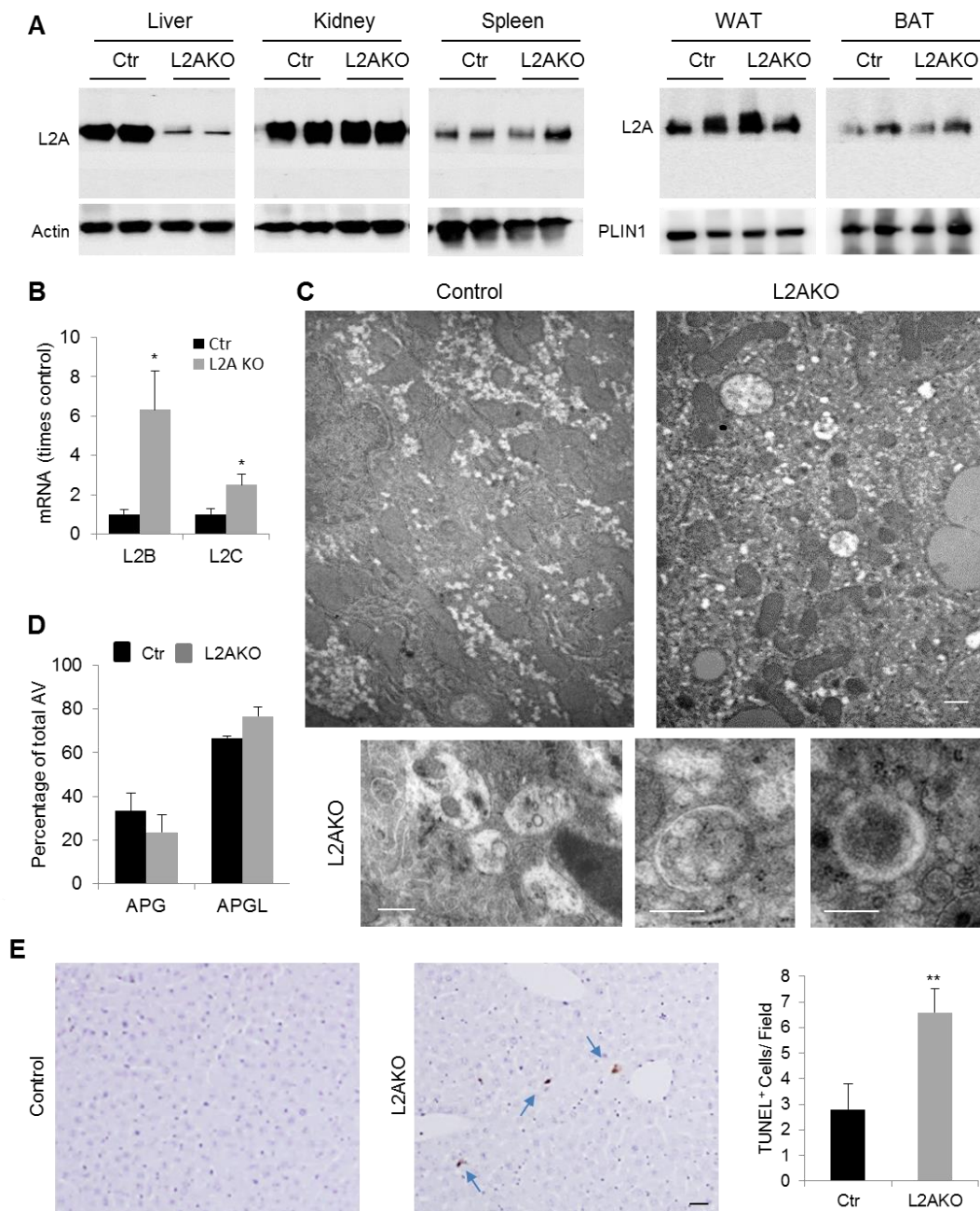


Figure S1; relates to Fig. 1: The lysosomal/autophagic system in liver-specific L2AKO mice. (A) Immunoblot for LAMP-2A (L2A) in homogenates of the indicated tissues from control (Ctrl) and Albumin-Cre-L2A^{fl/fl} (L2AKO) mice. Two different animals are shown per group. **(B)** Quantification by RT-PCR of LAMP-2B and LAMP-2C mRNA levels in livers from Ctrl and L2AKO mice, n=4. **(C)** Representative electron micrographs of livers from starved Ctrl and L2AKO mice. Insets below show higher magnification images of autophagosomes and autophagolysosomes in L2AKO mice. (Scale bar, 0.5 μ m). **(D)** Percentage of autophagic vacuoles identified as autophagosomes (APG) or autophagolysosomes (APGL) through morphometric quantification of electron micrographs as the ones shown in **C**, n=4. **(E)** TUNEL staining in livers from Ctrl and L2AKO mice. *Left*: Representative sections. Arrows: apoptotic cells. *Right*: Quantification of the average number of TUNEL positive cells per field. (Scale bar, 20 μ m), n=4. All values are mean+s.e.m. Differences with Ctrl are significant for * P < 0.05; ** P<0.001.

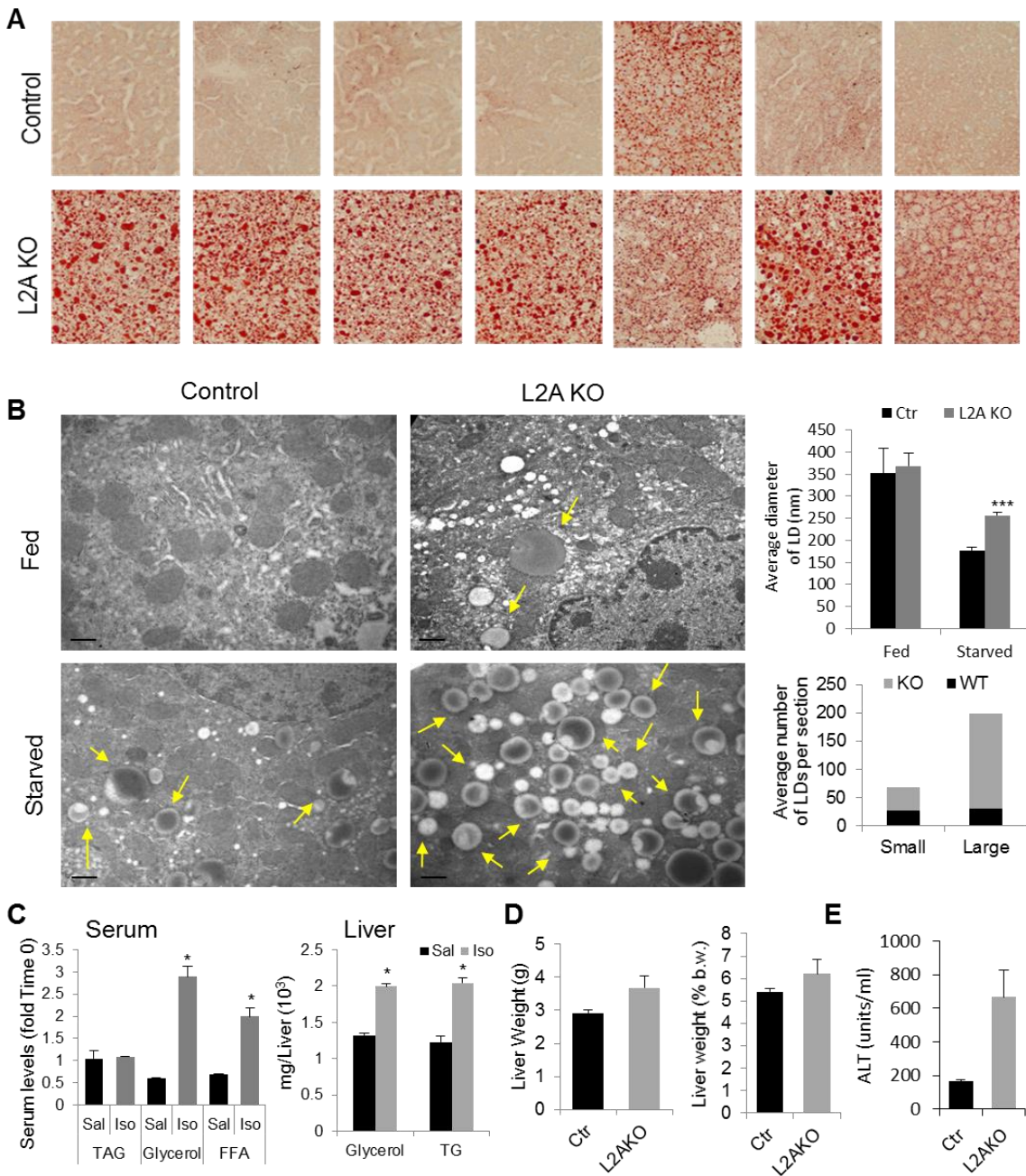


Figure S2; relates to Fig. 2: Hepatosteatosis in liver-specific L2AKO mice. (A) Oil Red O (ORO) staining of liver sections from 24h starved control (Ctr) and Albumin-Cre-L2A^{ff} (L2AKO) mice. Seven different animals from each group are shown to illustrate individual variability. (B) Electron micrographs of lipid droplet (LD)-enriched areas in livers of normally fed or 24h starved Ctr and L2AKO mice. Arrows: LD. Right: Average LD diameter (top) and number of small (<math><0.05 \mu\text{m}</math>) and large (> 0.05 $\mu\text{m}</math>) LD per section (bottom), calculated through morphometric analysis of micrographs as the ones shown here, $n=4$. (C) Left: Serum levels of free fatty acids (FFA), glycerol and triglyceride (TG) 15 minutes after saline (Sal) or isoproterenol (Iso) injection of Ctr mice, $n=2$. Right: Liver glycerol and TG measured 24h after two injections of either Sal or Iso, $n=2$. (D) Total liver weight (left) or relative to body weight (b.w.) (right) in Ctr and L2AKO mice after 16 weeks on a high-fat diet, $n=3-4$. (E) Serum levels of alanine aminotransferase (ALT) in the same mouse groups, $n=3$. All values are mean + s.e.m. Differences with Ctr are significant for * $P < 0.05$, ** $P < 0.01$, and *** $P < 0.001$.$

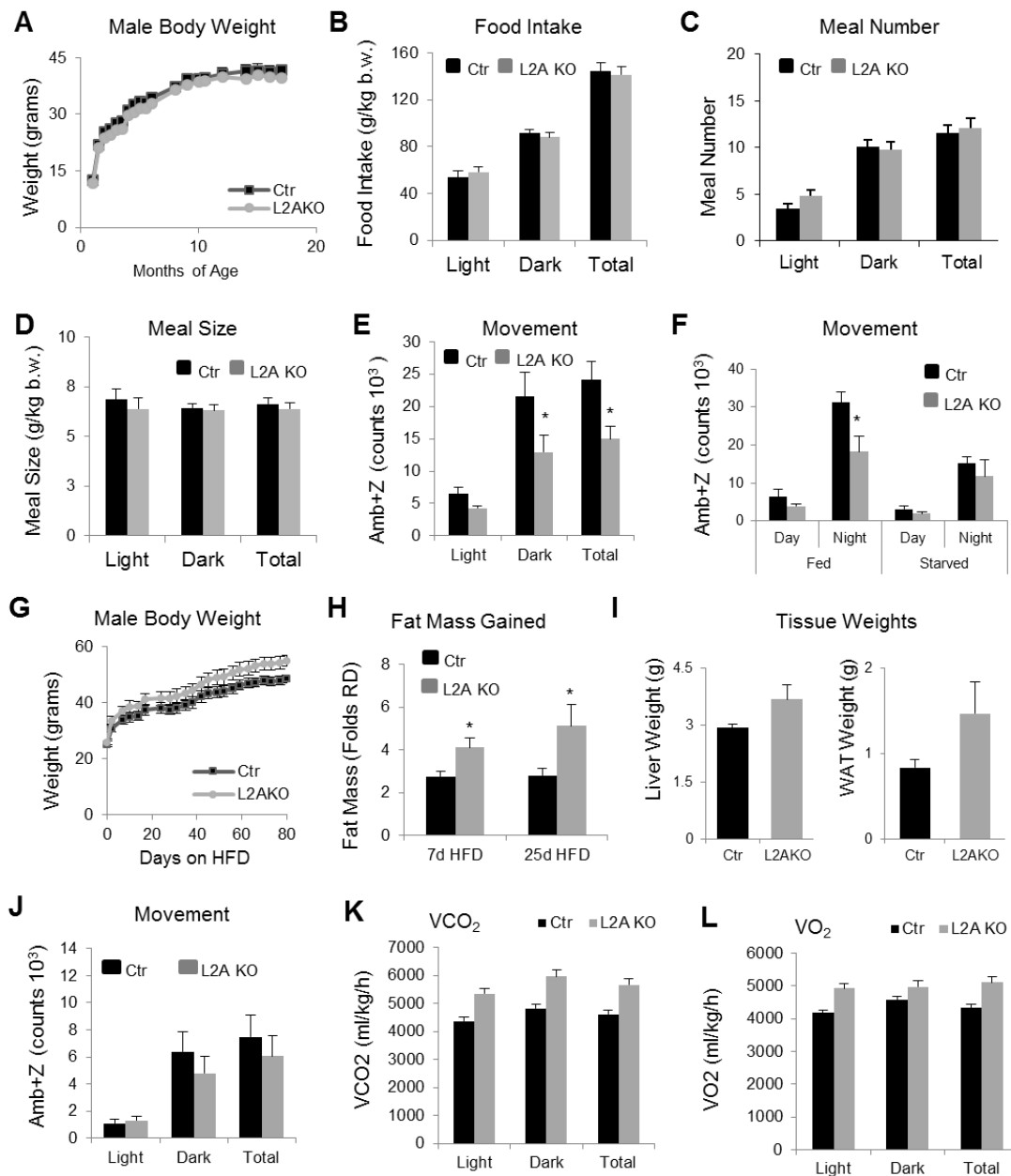


Figure S3; relates to Fig. 3: Systemic energetic balance in liver-specific L2AKO mice. (A) Changes in body weight with age in control (Ctr) and Albumin-Cre-L2A^{ff} (L2AKO) male mice, n=11-22. (B-D) Food intake (B), meal number (C) and average meal size (D) of the same groups of animals at 4 months of age during the light or dark cycles or throughout a 24h period (Total), n=8. (E, F) Average values of the ambulatory activity in three axes (Amb+Z) of Ctr and L2AKO mice normally fed (E) or starved for a 24h period (F). (G) Changes in body weight with age in Ctr and L2AKO mice fed a high fat diet (HFD) for 16 weeks, n=6-7. (H) Fat mass gained by Ctr and L2AKO mice at the indicated times in the HFD. Values are expressed relative to fat mass gained in Ctr during the same time, n=6-7. (I) Total weight of livers (left) and perigonadal white adipose tissue (WAT, right) from Ctr and L2AKO mice after 16 weeks in HFD, n=3. (J) Average value during the light or dark cycles or throughout a 24h period (total), of the ambulatory activity in three axes (Amb+Z) of the same group of animals as in G, n=4. (K,L) Average values of oxygen consumption (VO₂) and carbon dioxide production (VCO₂) in Ctr and L2AKO fed mice, n=8. All values are mean + s.e.m. Differences with Ctr were significant for * P < 0.05.

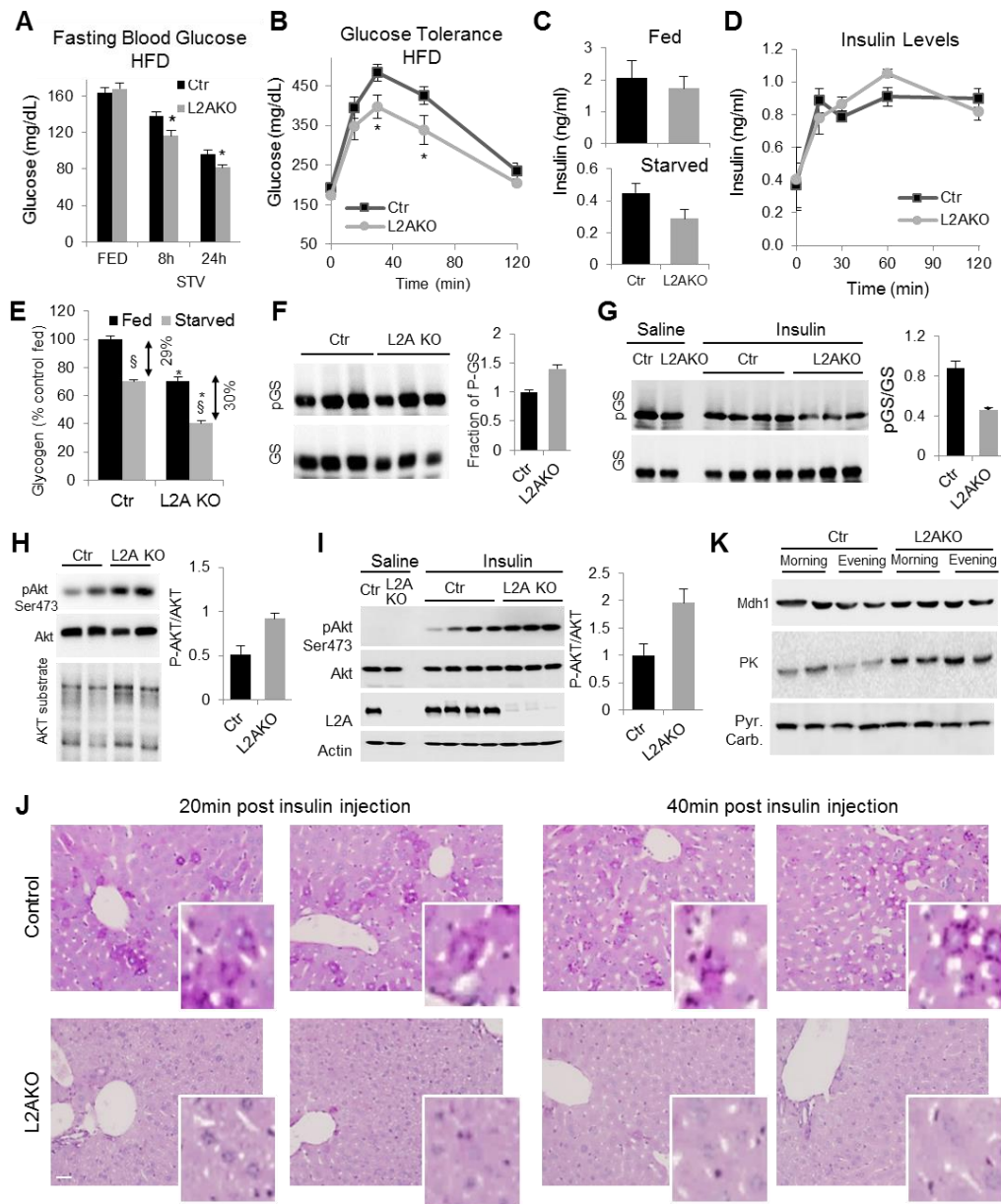


Figure S4; relates to Fig. 4: Carbohydrate metabolism in liver-specific L2AKO mice. (A) Blood glucose levels in fed and 8h or 24h starved control (Ctr) and Albumin-Cre-L2A^{fl/fl} (L2AKO) mice fed a high fat diet (HFD) for 16 weeks, n=6-7. **(B)** Glucose tolerance tests after overnight fasting in the same animal groups as in **A**, n=6. **(C)** Serum insulin levels in fed and 24h starved Ctr and L2AKO mice, fed n=7; starved n=13-24. **(D)** Serum insulin levels during the glucose tolerance test shown in Fig. 4B, n=4. **(E)** Changes in glycogen content in the livers of the indicated animals expressed as percentage of the glycogen content in fed Ctr mice, n=4. **(F-H)** Immunoblot for glycogen synthase (GS) and its phosphorylated variant (pGS) **(F,G)** or for AKT, AKT phosphorylated at Ser473 (pAKT) and AKT substrates **(H,I)** of liver homogenates from Ctr and L2AKO mice fed **(F,H)** or overnight starved and injected with insulin (2 mU g⁻¹) or saline 20 min before tissue harvesting **(G,I)**. *Right*: ratio of pGS relative total GS **(F,G)** or pAKT relative to total ATK **(H,I)** in the same samples, n=3-4. **(J)** Periodic acid-Schiff (PAS) staining of liver sections from overnight starved Ctr and L2AKO mice at the indicated times after the insulin bolus. Two different animals shown (scale bar, 50 μ m). **(K)** Immunoblot in liver homogenates collected in the morning or evening (7pm; before lights go off) from *ad libitum* fed Ctr and L2AKO mice, n=2. PK, pyruvate kinase; Mdh1, malate dehydrogenase 1, cytoplasmic; Pyr. Carb., pyruvate carboxylase. All values are mean + s.e.m. Differences with Ctr (*) or with fed (§) are significant for P < 0.05.

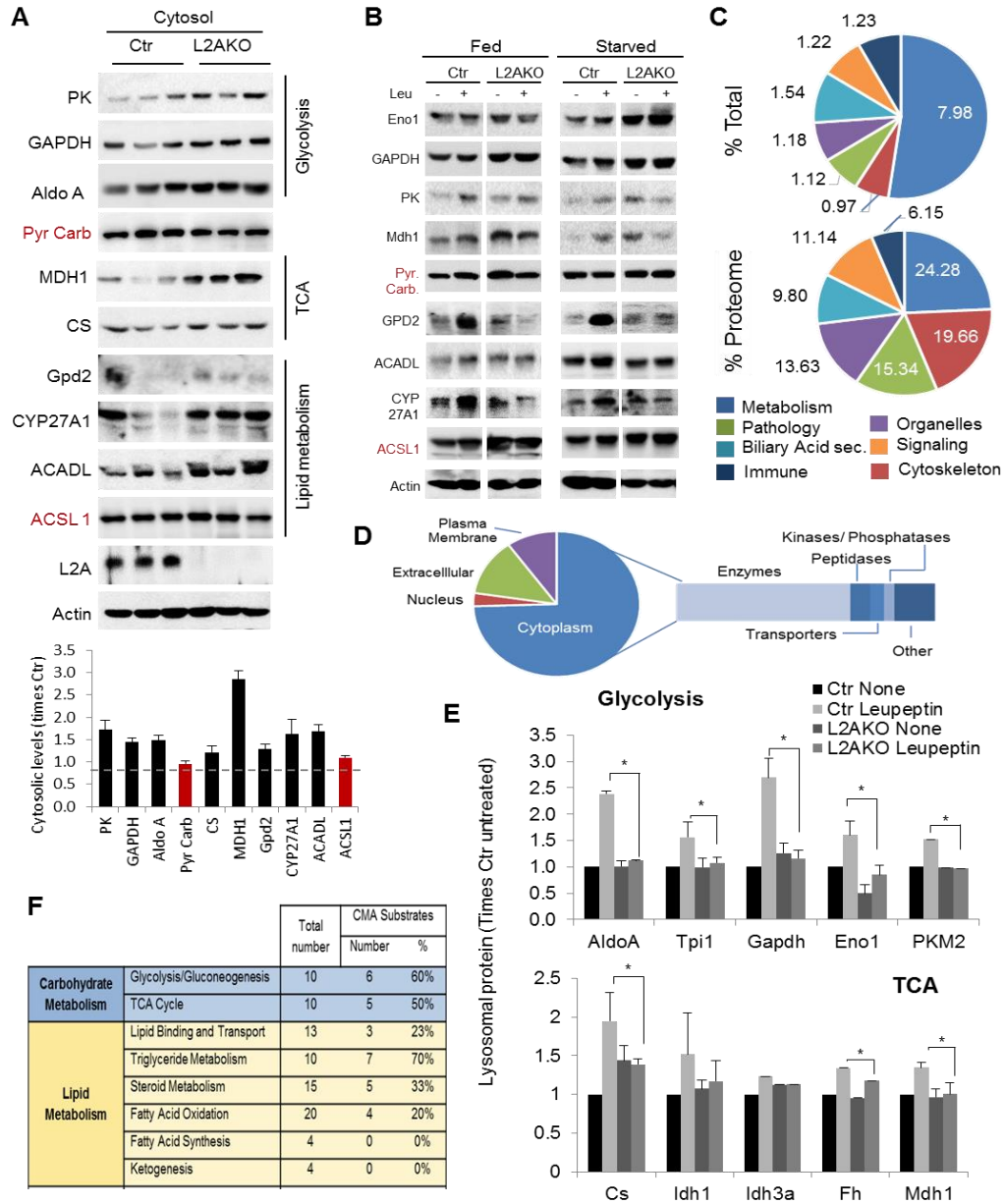


Figure S5; relates to Fig. 5: Chaperone-mediated autophagy in the turnover of liver enzymes involved in carbohydrate metabolism. (A) Immunoblot for the indicated enzymes in cytosolic fractions from liver of three different 24h starved control (Ctr) and Albumin-Cre-L2A^{fl/fl} (L2AKO) mice. *Bottom*: Levels of cytosolic enzymes in L2AKO mice relative to Ctr calculated by densitometric quantification, n=3. Enzymes without a CMA-targeting motif are in red. (B) Immunoblot for the indicated enzymes in livers of fed or 24h starved Ctr and L2AKO mice treated or not with leupeptin (Leu) 2h prior to tissue harvesting. Quantification shown in Fig. 5F and 7D. (C) *Top*: Percentage of proteins in each of the indicated cellular processes identified as CMA substrates through the comparative proteomic analysis as described in Fig. 5B. *Bottom*: Distribution of the total liver proteome among the functional groups used in the proteomic analysis. (D) Subcellular distribution (pie chart) and functional classification (bar chart) of the proteins identified as CMA substrates. (E) Levels of glycolytic (top) and TCA cycle (bottom) enzymes in the mice groups used for the proteomic analysis. Values are expressed relative to values in untreated Ctr mice, n=3. (F) Number and percentage of proteins involved in carbohydrate and lipid metabolism identified as CMA substrates through immunoblot and through the comparative proteomic analysis. All values are mean + s.e.m. Differences with Ctr (*) or with fed (§) are significant for P < 0.05.

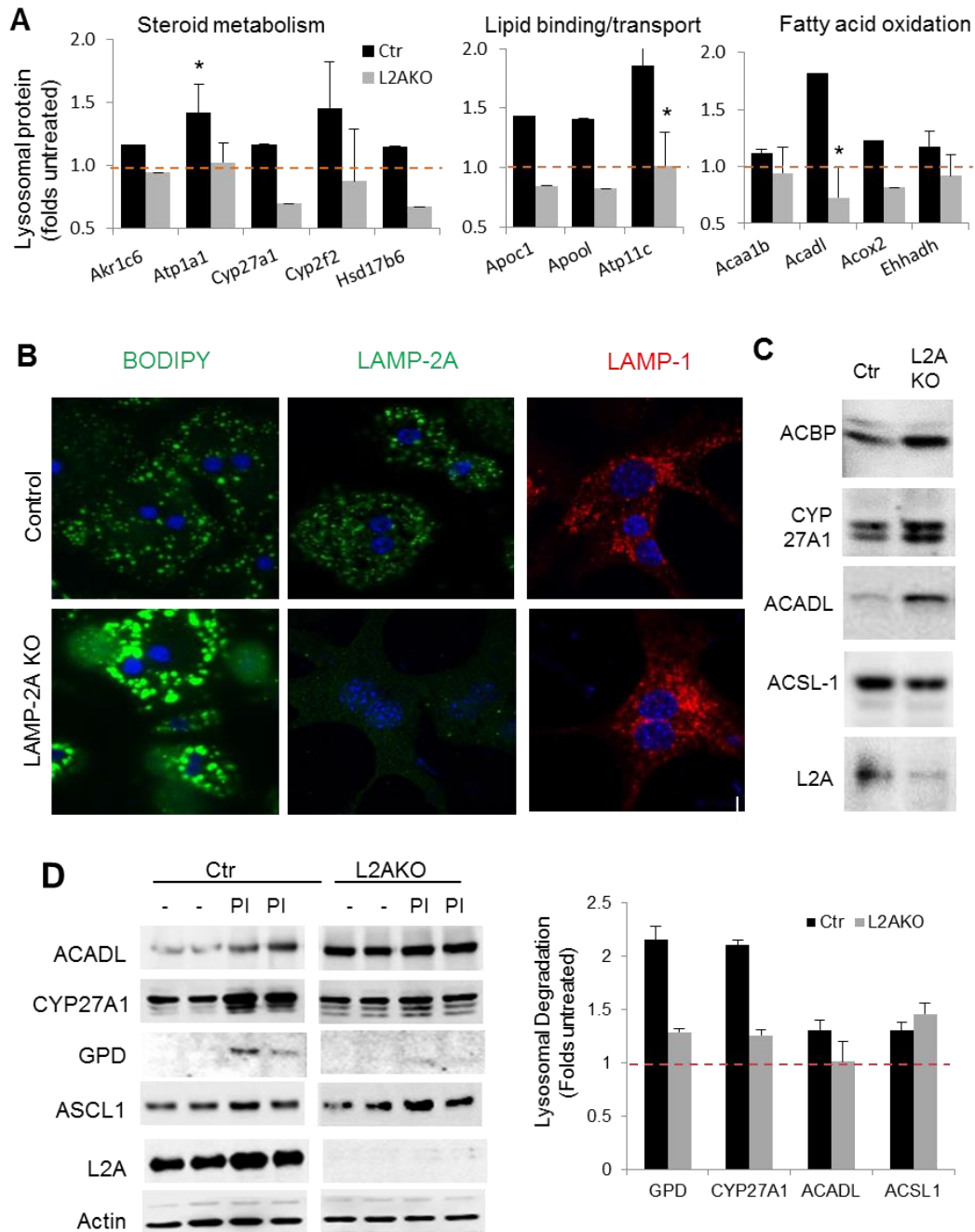


Figure S6; relates to Fig. 7: Metabolic changes in cells with compromised chaperone-mediated autophagy. (A) Folds increase in the levels of the indicated proteins related to lipid metabolism in lysosomes after leupeptin treatment as determined in the comparative proteomic analysis. Orange line indicates values in samples from Ctr untreated mice (arbitrary value of 1), $n=3$. Akr1c6: Aldo-keto reductase 1C6; Cyp27A1: Sterol 27-hydroxylase; Apoc1: Apolipoprotein C1; Apool: Apolipoprotein O-like; Acaa1b: Acetyl-CoA acyltransferase 1B; Acadl: Acyl-CoA dehydrogenase, long-chain; Acox2: Acyl-CoA oxidase 2; Ehhadh: Peroxisomal enoyl-CoA hydratase. All values are mean + s.e.m. Differences with Ctr (*) are significant for $P < 0.05$. (B) Lipid droplets highlighted by BOPIPY staining and endo/lysosomal compartments highlighted by immunostaining for LAMP-2A or LAMP-1 in primary hepatocytes isolated from Ctr or L2AKO mice. (C, D) Immunoblot for indicated lipid metabolism enzymes in primary hepatocytes under basal conditions (C) or after treatment with or without leupeptin (D) for 2h. Right: Densitometric quantification ($n=2$).

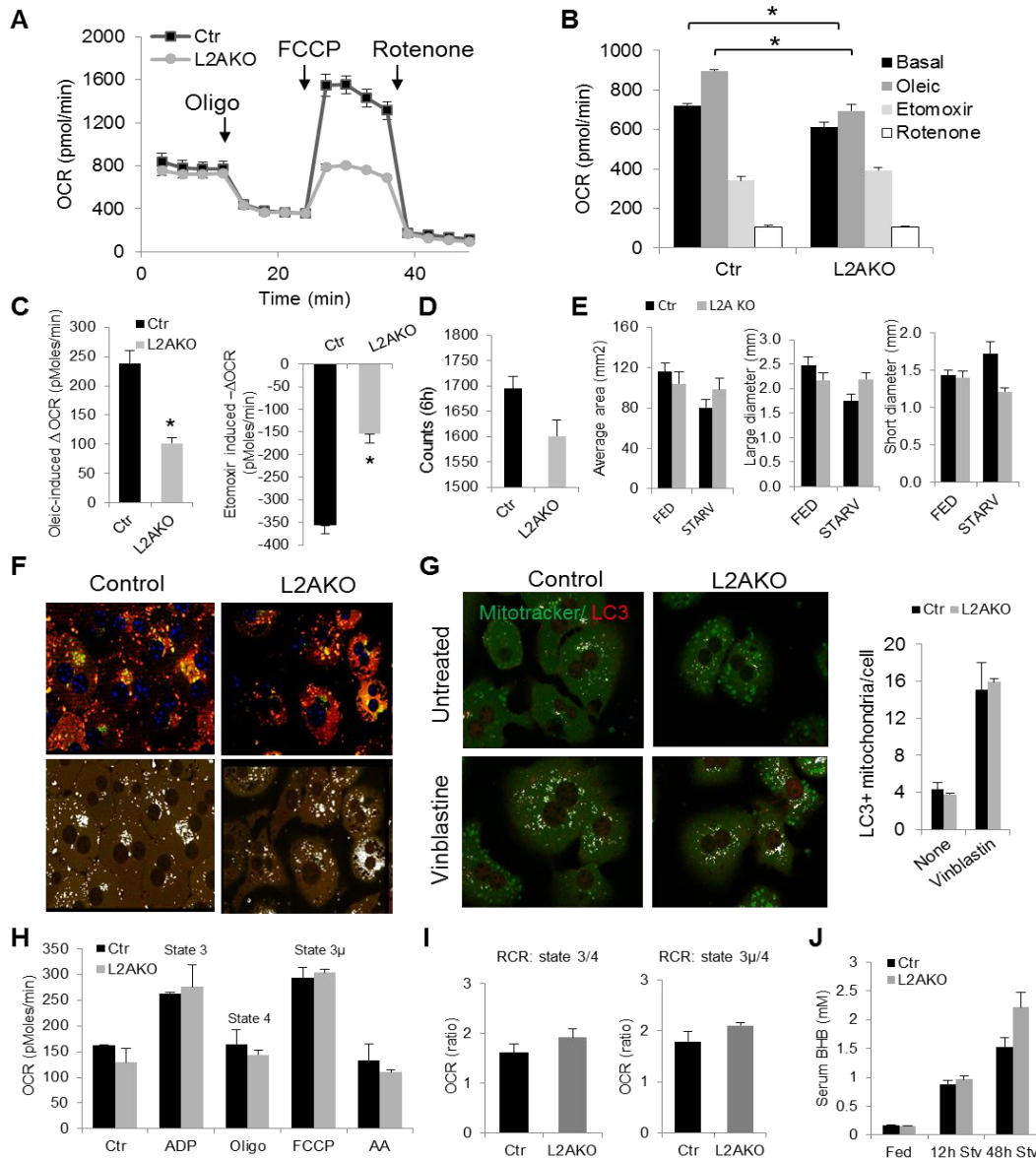


Figure S7; relates to Fig. 7: Mitochondrial function in hepatocytes with compromised chaperone-mediated autophagy. (A) Oxygen consumption rates (OCR) measured in hepatocytes isolated from Ctr or L2AKO mice before and after addition of inhibitors or activators of mitochondrial respiration, n=6. (B) OCR of hepatocytes from Ctr and L2AKO mice incubated in serum-depleted media overnight and in glucose-free media one hour prior to measurement in the presence of the indicated compounds, n=4. (C) Oleic-induced increase and etomoxir-induced reduction in OCR in the same cells. (D) β -oxidation in the same cells measured as the release of ^3H after 6h of labeling with ^3H -palmitate, n=3. (E) Average mitochondrial area, large and short diameter, and intensity of mitochondria in livers from Ctr and L2AKO mice. Values were obtained from morphometric analysis of electron micrographs as the ones shown in Fig. S1C and S2B, n= 3-4 different fields and >50 mitochondria. (F,G) Co-staining of isolated hepatocytes with MitoTracker-Green and Mito-CMXRos-Red (left) or MitoTracker-Green followed by anti-LAMP-1 (L1) (right) in the presence or absence of vinblastine. Colocalizing pixels are shown in white. *Right:* Quantification of LC3-positive mitochondria. (H) OCR of mitochondria isolated from Ctr and L2AKO mouse livers before and after treatment with activators and inhibitors of respiration, n=4. (I) Respiratory control ratios calculated from states 3 and 4 of mitochondrial respiration in (H), n=8. (J) Plasma ketone body levels (BHB: beta-hydroxybutyrate) in Ctr and L2AKO mice fed or starved for indicated period of time (n=4-7). All values are mean + s.e.m. Differences with Ctr (*) are significant for $P < 0.05$.